



TITLE:

RF Characteristics of 433.3-MHz Proton RFQ Linac

AUTHOR(S):

Sawamura, M.; Okamoto, H.; Iwashita, Y.;
Fukunaga, K.; Inoue, M.; Takekoshi, H.

CITATION:

Sawamura, M. ...[et al]. RF Characteristics of 433.3-MHz Proton RFQ Linac. Bulletin of the
Institute for Chemical Research, Kyoto University 1988, 66(1): 29-37

ISSUE DATE:

1988-03-29

URL:

<http://hdl.handle.net/2433/77214>

RIGHT:

RF Characteristics of 433.3-MHz Proton RFQ Linac

M. SAWAMURA, H. OKAMOTO, Y. IWASHITA, K. FUKUNAGA,
M. INOUE and H. TAKEKOSHI

Received February 1, 1988

A 433.3 MHz proton RFQ linac of four vane type is constructed. The vane length and the inner tank diameter are 2195 mm and 170.4 mm respectively. The quadrupole field balance is analyzed with the equivalent circuit. Twenty-four pick-up loops are used to measure the magnetic field. The field is tuned with twenty-four side tuners and good field balance between each quadrant is obtained. The intervening electrodes, which compensate the decrease of the intervane capacitance at the radial matcher, are tested to improve the longitudinal field distribution.

KEY WORDS: RFQ Linac/ Proton Linac/ Equivalent Circuit/ RF Measurement/

1. INTRODUCTION

A 7-MeV proton linac is now under construction at the Nuclear Science Research Facility, Institute for Chemical Research, Kyoto University.¹⁾ As the first stage of this linac, a four vane type radio-frequency quadrupole (RFQ) linac was constructed (Photo 1, 2, 3). The vane length and the inner tank diameter are 2195 mm and 170.4 mm respectively. It is under cold measurement.

The geometry of end regions of the RFQ cavity was found to be important to achieve the good longitudinal field distribution.²⁾ But the end tuners were not effective to adjust the field distribution of both end regions in our case. Thus we made end plates with movable end wall and an exchangeable nose to modify the geometry

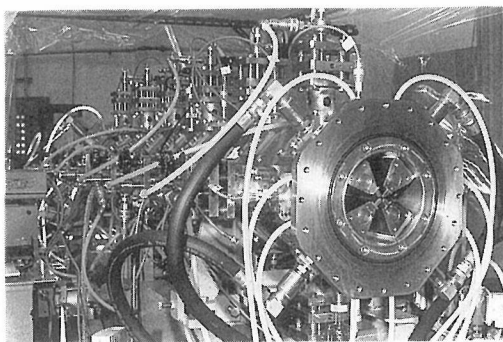


Photo 1. View of the RFQ tank.

沢村 勝, 岡本宏巳, 岩下芳久, 福永清二, 井上 信, 竹腰秀邦: Nuclear Science Research Facility, Institute for Chemical Research, Kyoto University.

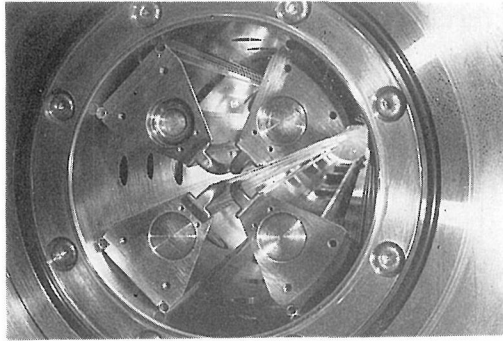


Photo 2. Inside view of the cavity from the entrance.

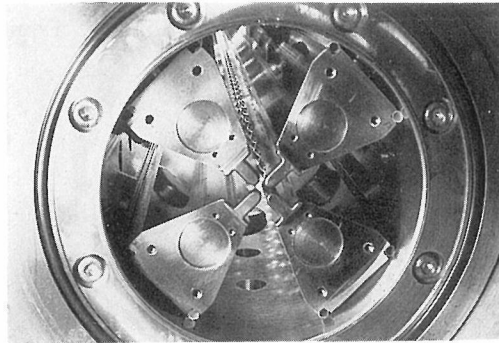


Photo 3. Inside view of the cavity from the exit.

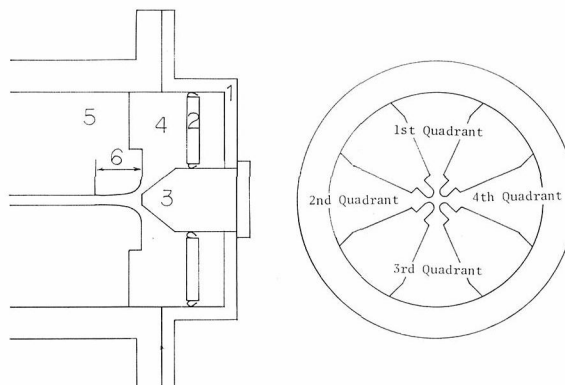


Fig. 1. The geometry of the end region near the entrance.
 1: end plate 2: movable end wall 3: nose 4: end region 5: vane 6: radial matcher

of end regions (Fig. 1). The equivalent circuit analysis and the experimental results are described in the following sections.

2. EQUIVALENT CIRCUIT ANALYSIS

An equivalent circuit analysis in the transverse plane is helpful to understand the field tuning characteristics of side tuners. The equivalent circuit is shown in Fig. 2³⁾. C_{0n} represents the intervane capacitance of the n-th quadrant. C_{13} and C_{24} represent the capacitances between two opposing vanes. L_{0n} represents the inductance of the n-th quadrant. Decrease of L_{0n} corresponds to insertion of the side tuner of n-th quadrant. The frequency and field strength of each quadrant are simulated by the eigen-value problem of the equivalent circuit. The equation of this eigen-value problem is as follows;

$$\begin{bmatrix} \frac{1}{L_{01}} + \frac{1}{L_{04}} & \frac{1}{L_{04}} & \frac{1}{L_{04}} \\ \frac{1}{L_{04}} & \frac{1}{L_{02}} + \frac{1}{L_{04}} & \frac{1}{L_{04}} \\ \frac{1}{L_{04}} & \frac{1}{L_{04}} & \frac{1}{L_{03}} + \frac{1}{L_{04}} \end{bmatrix} \begin{bmatrix} E_1 \\ E_2 \\ E_3 \end{bmatrix} = \omega^2 \begin{bmatrix} C_{01} + C_{13} + C_{04} & C_{13} + C_{04} & C_{04} \\ C_{13} + C_{04} & C_{02} + C_{13} + C_{24} + C_{04} & C_{24} + C_{04} \\ C_{04} & C_{24} + C_{04} & C_{03} + C_{24} + C_{04} \end{bmatrix} \begin{bmatrix} E_1 \\ E_2 \\ E_3 \end{bmatrix}$$

$$E_4 = -E_1 - E_2 - E_3$$

where ω is angular frequency and E_n is the intervane voltage of the n-th quadrant.

We calculate quadrupole field balance at three sets of tuner length when $C_{01} = C_{02} = C_{03} = C_{04} = C_0$ and $C_{13} = C_{24} = C_1$; as follows.

- 1) All the tuners have the same length. ($L_{01} = L_{02} = L_{03} = L_{04} = L_0$)

$$\omega^2 = \frac{1}{L_0 C_0}$$

$$E_1 = -E_2 = E_3 = -E_4$$

This represents ideal quadrupole mode.

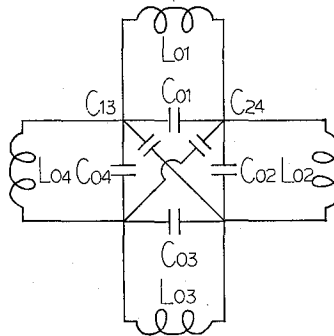


Fig. 2. Equivalent circuit in the transverse plane of the RFQ cavity.

- 2) Tuner length is same in opposing quadrants, but different in adjacent ones.
 $(L_{02}=L_{04}=L_0, L_{01}=L_{03}=L_1=L_0+dL)$

$$\omega^2 = \frac{L_0+L_1}{2L_0L_1C_0} \div \frac{1}{L_0C_0} \left(1 - \frac{dL}{2L_0}\right),$$

$$E_1 = -E_2 = E_3 = -E_4.$$

This suggests that the tuners inserted in opposing quadrants by the same length ($dL < 0$) increases the frequency and the field balance remains unchanged.

- 3) Only one tuner length is different from the others. ($L_{02}=L_{03}=L_{04}=L_0, L_{01}=L_1=L_0+dL$)

$$\omega^2 \div \frac{1}{L_0C_0} \left(1 - \frac{dL}{4L_0}\right),$$

$$E_2=E_4=E, E_1 \div -\left(1 - \frac{C_0}{2L_0C_1}dL\right)E, E_3 \div -\left(1 + \frac{C_0}{2L_0C_1}dL\right)E,$$

$$|E_1| < |E_2| = |E_4| < |E_3| \quad (dL > 0),$$

$$|E_1| > |E_2| = |E_4| > |E_3| \quad (dL < 0).$$

when the tuner in the n-th quadrant is inserted ($dL < 0$), the field of the n-th quadrant increases and the opposing one decreases while the others remain unchanged.

3. FIELD TUNING

3.1 Method of Measurement

There are two methods to measure the field distribution. One is the bead perturbation method, which is very time consuming. The other is the magnetic field measurement by pick-up loops. The rough field distribution can be determined quickly by this method. In our experiments the latter method was adopted for saving time.

Six pick-up loops were installed in each quadrant. The coupling coefficient is in the order of 10^{-4} and is small enough not to disturb the distribution. Each pick-up loop had a 6dB attenuator to reduce the standing wave on the coaxial cable. The coupling coefficient of each pick-up loop was calibrated by measuring the output power at the same pick-up hole. A twenty-four to one multiplexer was made to select a pick-up loop.

3.2. Field Distribution

The RFQ cavity had six side tuners of 4 cm diameter in each quadrant. All side tuners had an adjustable range of -6 mm to $+20$ mm from the tank inner wall toward beam axis. RF power was fed by the loop coupler located in the middle of the 4th quadrant, where the high power loop coupler should be located. The coupling coefficient was in the order of 10^{-2} .

All side tuners were set to be the same length of 1 mm at the beginning. The measured field distribution on this condition is shown in Fig. 3. Then the field was tuned by adjusting the side tuners step by step on the basis of the results from the equivalent circuit analysis. Tuned field distribution is shown in Fig. 4. The field

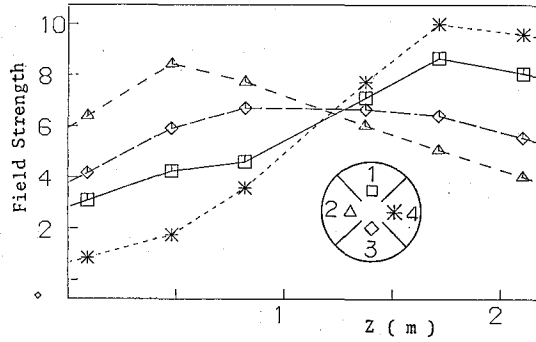


Fig. 3. The field distribution (arbitrary unit) when the length of all side tuners is 1 mm.

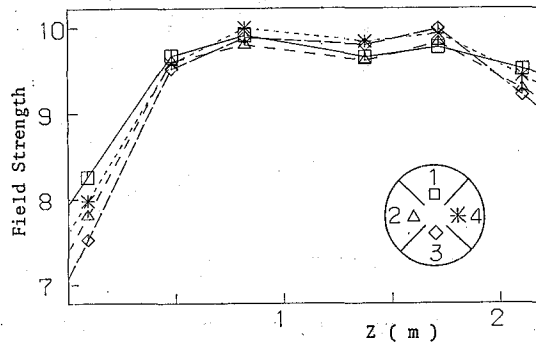


Fig. 4. The field distribution (arbitrary unit) after tuning.

differences between each quadrant were within 3% at every pick-up loop position except the entrance. The longitudinal field deviation was within 4.7% except near the entrance and the exit.

3.3 Expansion of End Region

One reason of the field drop near the entrance and the exit is the higher intrinsic frequency of the end regions due to the less volume. Figure 5 shows the longitudinal field distribution as a function of the distance between the vane and the end wall. These results show the fields near the exit are improved by increasing the volume of end region, but those near the entrance are not improved very much.

3.4 Intervening Electrode between Vanes

The RFQ linac generally consists of four sections called such as radial matcher, shaper, gentle buncher and accelerator. At the radial matcher the bore radius increases at the entrance and the intervane capacitance is less than that of the other sections. Therefore if the inductance is constant all over the length, the intrinsic frequency is higher at the radial matcher. It is possible to increase the inductance by removing the vane base at end. Unfortunately the existing cut at the end of the vane base is not enough to compensate the effect of the decreased capacitance. This causes the field drop near the entrance of the RFQ linac.

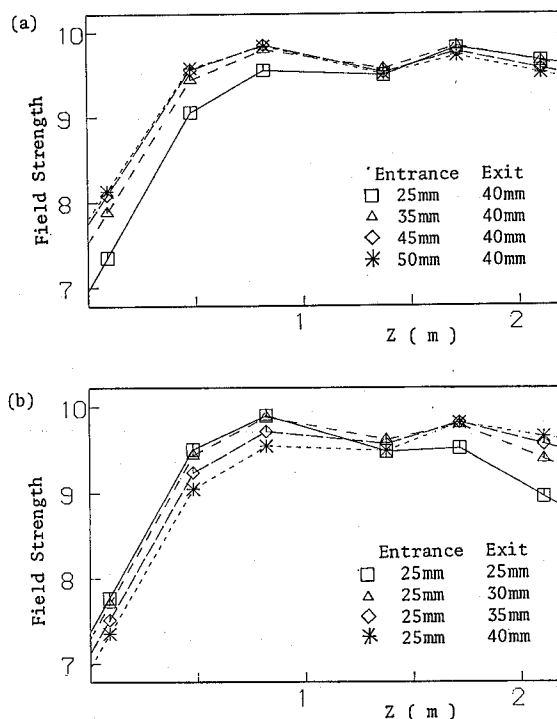


Fig. 5. The field strength (arbitrary unit) as a function of the distance between the end of vanes and the end wall.
(a) changing the entrance side distance. (b) changing the exit side distance.

It is difficult to cut off the vane base any more in order to increase the inductance. Following idea was tested to increase the capacitance between the adjacent vanes. A cone was inserted from the nose in the middle of each quadrant as an intervening electrode as shown in Fig. 6. The position and the radius of the cone were determined by SUPERFISH calculations so that the resonant frequency of the radial matcher would be kept constant. The relations between the position and the radius of cone are shown in Fig. 7 at several bore radii. In consideration of spark problem, the cones were set at the radius of 15.55 mm from the beam axis. The tuned field distribution with the intervening electrodes is shown in Fig. 8. In these measurements the distances between the vane and the end plate at the entrance and the exit were both

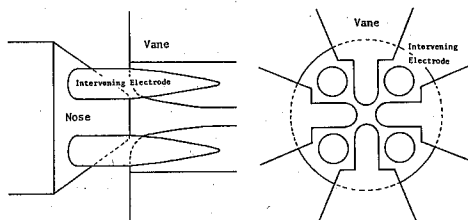


Fig. 6. Intervening electrodes.

RF Characteristics of 433.3-MHz Proton RFQ Linac

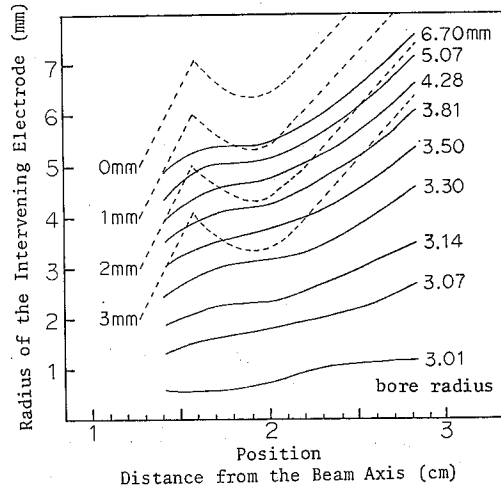


Fig. 7. The relation between the distance from the beam axis and the radius of the intervening electrode at several bore radii. The broken lines show a contour plot of the shortest distance between the vane surface and the intervening electrode.

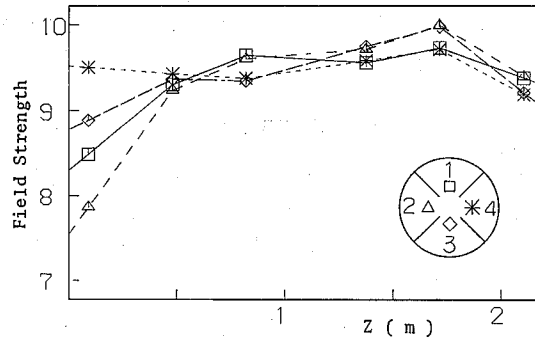


Fig. 8. The field distribution (arbitrary unit) after tuning with the intervening electrodes of the same length.

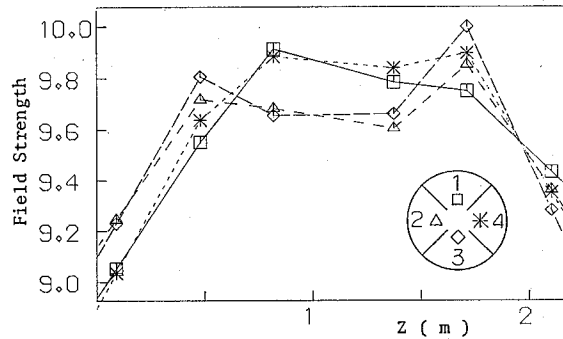


Fig. 9. The field distribution (arbitrary unit) after adjusting the length of the intervening electrodes.

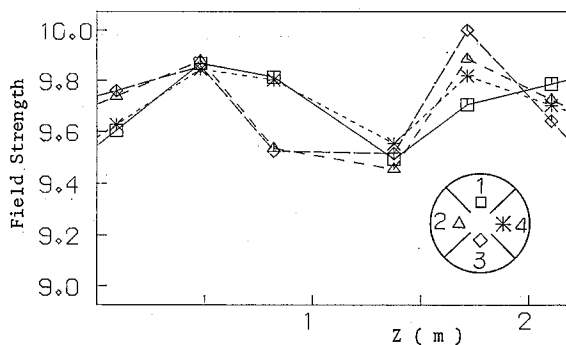


Fig. 10. The field distribution (arbitrary unit) after adjusting the volumes of end regions with the intervening electrodes.

25 mm. The field near the entrance of the 4th quadrant was strong and that of the 2nd was weak. This might be caused by the positioning error of the nose. It was thought that the distance between the cone and the vane in the 4th quadrant was smaller and that in the 2nd was larger than expected. The improved field distribution after adjusting the length of the cones is shown in Fig. 9, and that after adjusting the volumes of end regions by moving the end walls is shown in Fig. 10. Finally the field differences between each quadrant became within 3% and the longitudinal deviation became within 5.5% including both ends as shown in Fig. 10.

4. MODE DISTRIBUTION

The resonant frequencies of various modes are shown in Fig. 11. TE_{11n} mode has two resonant frequencies according to the two choices of the direction. At the beginning the nearest resonant frequency to TE_{210} mode was $TE_{111(2,4)}$ (dominant in

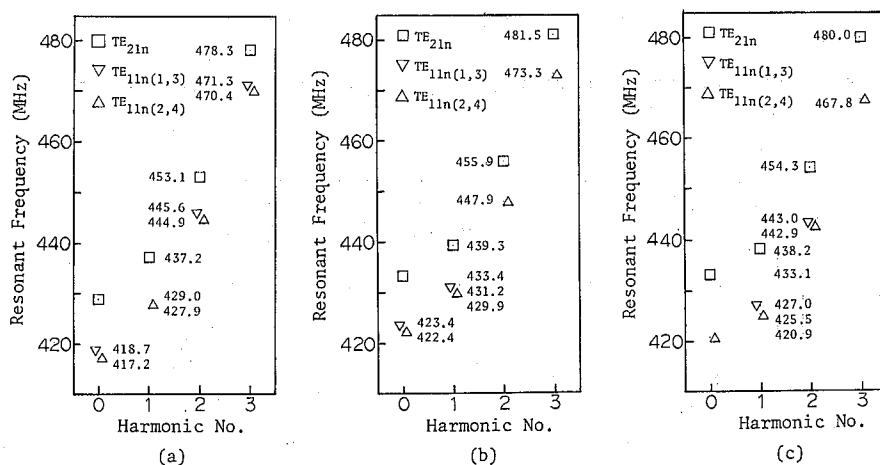


Fig. 11. The resonant frequencies.

(a) in the case of 1 mm length of all side tuners at the beginning. (b) after tuning without the intervening electrodes. (c) after adjusting the volume of end regions with the intervening electrodes.

the 2nd and 4th quadrants), and the measured frequencies were 427.9 MHz ($TE_{111(2,4)}$ mode) and 429.0 MHz (TE_{210} mode). The mode separation between TE_{210} mode and $TE_{111(2,4)}$ mode was 1.1 MHz. Because the resonant frequency of $TE_{111(1,3)}$ mode was about 0.5 MHz to 1 MHz higher than that of $TE_{111(2,4)}$ mode, $TE_{111(1,3)}$ mode, which was not found, was expected to be close to TE_{210} mode and be concealed by it.

After tuning without the intervening electrodes the nearest mode to TE_{210} mode (433.4 MHz) was $TE_{111(1,3)}$ mode (431.2 MHz), and the mode separation was 2.2 MHz. With the intervening electrodes the resonant frequencies of TE_{210} mode and $TE_{111(1,3)}$ mode were 433.1 MHz and 427.0 MHz respectively. The mode separation increased to 6.1 MHz and the nearest mode was TE_{211} mode (5.1 MHz above TE_{210} mode).

5. CONCLUSIONS AND DISCUSSIONS

The field differences between each quadrant within 3% were achieved by using the side tuners. Introducing enough volume at end regions and using the intervening electrode, the longitudinal field deviation within 6% could be achieved without inductive or capacitive end tuners, though the sharp cone tip of the intervening electrode might cause the spark problem at high power operation.

Characteristics of quadrupole field variations by changing the length of the side tuner were well explained by the equivalent circuit, but the longitudinal field variations were not yet analyzed sufficiently.

In our RFQ linac, the decrease of the intervane capacitance due to the increase of the modulation was compensated by making the modulation valley shallow as described in the previous paper.¹⁾ But it was necessary that the tuner length of the latter half was longer than that of the first half. It might be caused by the alignment error of the vanes and/or the overcompensation of the intervane capacitance.

REFERENCES

- (1) H. Okamoto et al., "Design of 433.3-MHz Proton RFQ Linac", *Bull. Inst. Chem. Res. Kyoto Univ.* vol. 65, No. 1 (1987).
- (2) T. Nakanishi et al., "RF Characteristics of a Four Vane Type RFQ Linac with a Single Loop Coupler", *Nucl. Instr. and Meth.*, A243 (1986).
- (3) J. M. Potter, "An RF Power Manifold for the Radio Frequency Quadrupole Linear Accelerator", *Proc. of the 1979 Linear Accel. Conf.*, (1979).